

INTRINSIC SEISMIC PROTECTION OF CANTILEVERED AND ANCHORED RETAINING STRUCTURES

Luigi CALLISTO¹ and Ilaria DEL BROCCO²

Abstract: This paper explores the possibility of applying the principles of capacity design to the seismic protection of embedded retaining structures. The study hinges on the analysis of the plastic mechanisms that may be activated by cantilevered and anchored retaining walls during strong motion while preserving the integrity of the structural members. Through a combination of numerical analyses and simple limit equilibrium calculations, it is shown that for the wall schemes considered in this work it is possible to derive the maximum internal forces that the structural members may undergo during a severe earthquake from the analysis of the relevant plastic mechanism. It is also shown that these internal forces do not depend on the amplitudes of seismic motion, but are related only to the strength of the dissipating elements of the system. For anchored walls, this approach indicates that the optimal way to limit the internal forces in the retaining wall is to design weak anchors, that during the seismic event may mobilise the strength at the contact of the soil with their injected active portion.

Introduction

Although the study of the interaction between a retaining structure and the surrounding soil is particularly complex under seismic conditions, for design purposes it could be unnecessary to predict the detailed dynamic behaviour of the system, but it may be sufficient to endow the structure with features that will ensure a desirable behaviour under a severe seismic event. To this respect, the seismic design of retaining structures can be regarded as a special case of the capacity design approach commonly employed in structural engineering: energy-dissipating elements of a plastic mechanism are chosen, that attain their full capacity during the seismic event; other elements are provided with sufficient strength capacity to ensure that the chosen plastic mechanism is maintained at near its full strength throughout the deformations that may occur. Following this line of thought, this paper shows that for cantilevered and anchored embedded retaining walls it is possible to use relatively simple pseudo-static tools, essentially based on the strength properties of the soil, to study the plastic mechanisms associated with the desired behaviour and to derive the internal forces that the structural elements are called to resist in order to fulfil the above requirement. In principle, the design of the structural members based this approach is intrinsically safe, in the sense that the internal forces derived from the analysis of a relevant plastic mechanism do not depend of the intensity of the earthquake. In the present paper, results of full dynamic analyses of the soil-structure interaction are discussed, in order to validate the proposed approach and to evidence its limitations.

Analysis methods

A fundamental part of this work consists of the analysis of the plastic mechanisms produced by intense seismic forces on a given retaining structure. This analysis is carried out with a finite-difference calculation (FLAC v. 5.1, Itasca, 2005) in which pseudo-static seismic forces are increased progressively up to the full mobilisation of the strength of the structure under examination. In this paper this approach is applied to embedded retaining walls of different geometry, either cantilevered or with a single anchor level. Callisto (2014) discusses the extension of the same procedure to walls restrained by a stiff prop level.

¹ Associate Professor, Sapienza University of Rome, Italy, luigi.callisto@uniroma1.it

² Doctoral student, Sapienza University of Rome, Italy, ilaria.delbrocco@uniroma1.it

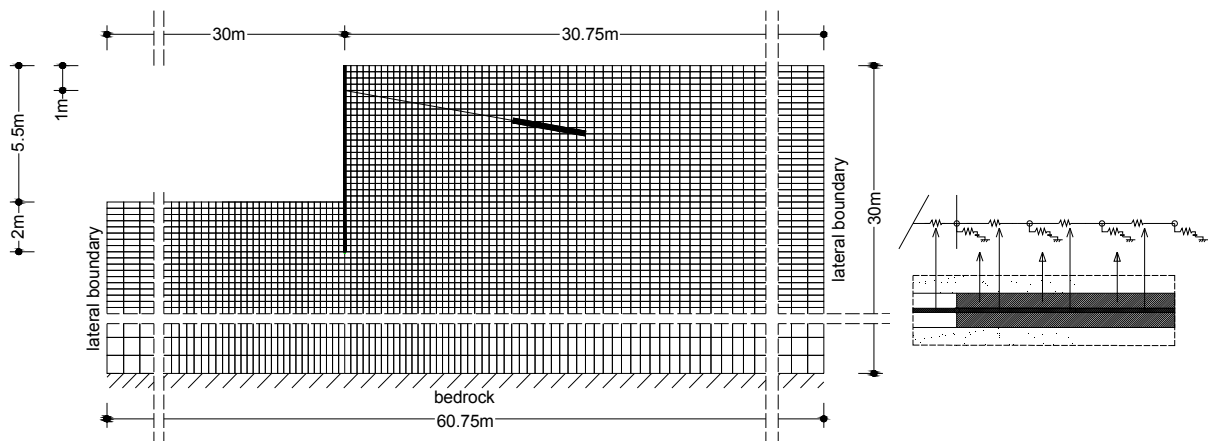


Figure 1. (a) finite difference grid used for anchored walls and (b) detail of the connection of the active portion of the anchor element to the grid nodes.

Figure 1 shows, as an example, one of the calculation grids employed for the analysis of the anchored walls. The excavation is carried out in a uniform and dry coarse-grained soil, characterised by an angle of shearing resistance φ , and by a small-strain shear modulus G_0 which is taken proportional to the square root of the mean effective stress p' . In the pseudo-static analyses an elastic-perfectly plastic soil model is used with a dilatancy angle equal to zero and an operational shear modulus equal to $0.3 G_0$. The retaining wall is described with beam elements, attached to the main grid through perfectly plastic interfaces elements with a reduced friction angle δ . For the anchored walls, the anchor level is described with cable elements that are connected to the finite difference grid through elastic-perfectly plastic interfaces (Fig. 1.b).

After having simulated the excavation sequence, the horizontal body forces, proportional to the gravitational forces through the seismic coefficient k_h , were increased progressively, searching iteratively the value of the critical seismic coefficient k_c that corresponds to the complete mobilisation of the strength of the system. All the analyses schemes yielded values of k_c significantly smaller than the limit value $k_h = \tan \varphi$, corresponding to the mobilisation of the shear strength in the entire model. Consistently, it was seen that under critical conditions most of the plastic strains concentrated in the vicinity of the excavation.

Some parametric studies were carried out to ascertain that the grid size is sufficiently fine. Checks were also made that, consistently with perfect plasticity results, the critical seismic coefficient and the ensuing plastic mechanism do not depend on the stiffness properties of both the soil and the structural elements.

Since the structural members (the retaining wall and the anchor elements) are modelled as linearly elastic, any plastic mechanism activated by the pseudo-static seismic forces derives from the mobilisation of the soil strength only, either within the soil mass, or at the contact to the wall and to the active portion of the anchor). The internal forces acting in the structural members under these critical conditions can be deemed representative of the maximum internal forces that occur during a severe seismic event in the time instant when the plastic mechanisms are temporarily activated (Callisto & Soccodato 2010).

When the overall strength of the system is attained, a portion of the soil accelerates and the grid deformations increase indefinitely. The corresponding deformation pattern of the grid can be interpreted with sufficient accuracy as an assembly of rigid bodies that slide along

contact surfaces. Therefore, specific plastic mechanisms can be extracted from the results of the finite-difference calculations and analysed with a simple limit equilibrium approach.

Results obtained with the pseudo-static procedure were compared to those resulting from dynamic soil-structure interaction analyses. These were carried out on the same plane-strain finite difference models adopted in the pseudo-static numerical analyses, activating the FLAC free-field dynamic conditions at their lateral boundaries. The dynamic analyses follow the methodology outlined in the paper by Callisto & Soccodato (2010), to which the reader is referred for details not included in the present description.

The cyclic behaviour of the soil was described through the hysteretic damping model implemented in FLAC, which is essentially an extension to two-dimensions of the non-linear soil models that describe the unloading-reloading stress-strain cycles with the Masing (1926) rules. The backbone curve for this model was calibrated to reproduce the Seed and Idriss (1970) modulus decay curve for coarse-grained materials. The bending stiffness of the beam elements correspond to a retaining wall made of 0.6 m diameter r.c. piles with a 0.7 m spacing.

The analyses included a static stage, in which the soil excavation was modelled in steps and the soil behaviour was elastic-perfectly plastic. In the subsequent dynamic stage, the hysteretic soil model was activated, and time-histories $a(t)$ of the horizontal acceleration were applied to the bottom boundary, while the FLAC free-field conditions were imposed at the lateral boundaries of the finite difference grid. A seismic input was selected that was sufficiently intense to activate the plastic mechanism of each retaining wall. To this purpose, the Tolmezzo record (as discussed by Callisto & Soccodato, 2010) was used in the analyses of the cantilevered walls; for the anchored wall, the acceleration amplitudes of this record were scaled by a factor of two to provide an effective activation of the corresponding plastic mechanisms.

Cantilevered walls

Figure 2 illustrates, as an example, the plastic mechanism obtained for a cantilevered wall with $H = 4$ m, $d = 4$ m, $\varphi = 35^\circ$ and $\delta = 20^\circ$, and specifically the displacement pattern (Fig. 2.a) and the soil zones that have reached their shear strength τ_f (Fig. 2.b). The mechanism is associated to a well-defined rotation of the wall around a point close to the toe; distinct active and passive wedges are visible behind and in front of the wall. The normal stresses σ_h at the soil-wall contact obtained from the pseudo-static analysis and the resulting bending moments

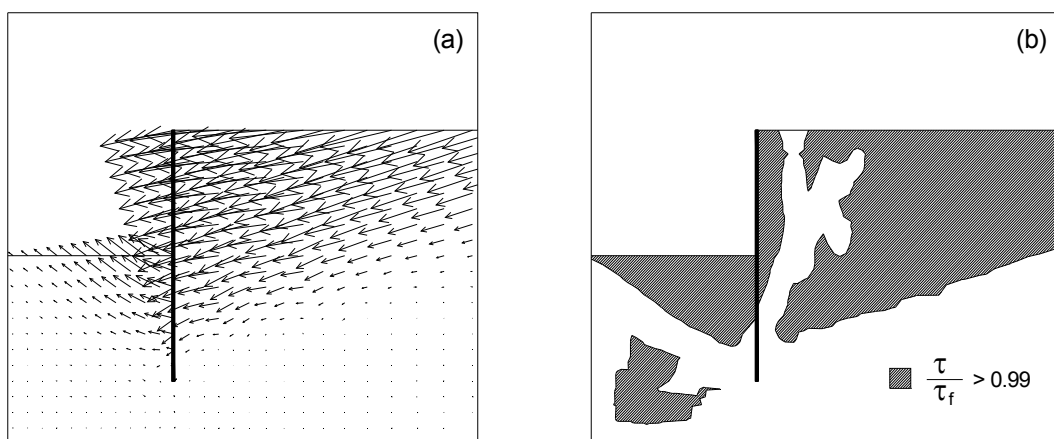


Figure 2. Cantilevered wall: (a) plastic mechanism; (b) soil zones with fully mobilised strength.

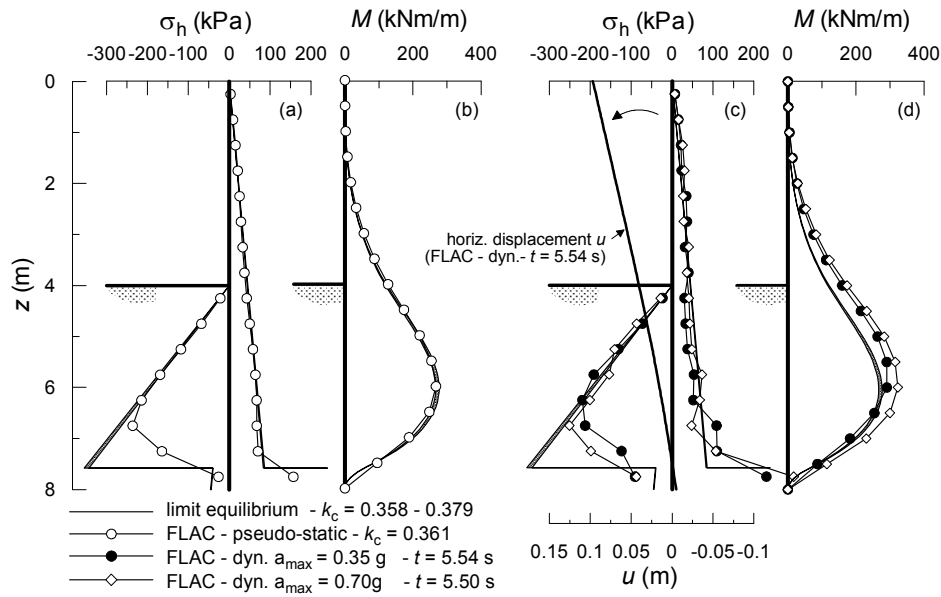


Figure 3. Distribution of horizontal contact stresses, bending moments, and wall displacements for the reference cantilevered wall: (a, b) pseudo-static analysis; (c, d) dynamic analysis (Tolmezzo record).

in the retaining wall are shown in Figure 3(a,b) with open symbols. For this case, the critical seismic coefficient is $k_c = 0.361$ and the maximum bending moment is $M_{max} = 267$ kNm/m. The present plastic mechanism can be studied with an iterative calculation based on limit equilibrium, assuming that it consists of a rigid rotation of the wall about a point close to its toe. Using either the lower-bound stress distribution proposed by Lancellotta (2007) or the Chang (1981) upper-bound kinematic approach, and searching iteratively for the seismic coefficient that ensures rotational and translational equilibrium of the wall, one obtains values of k_c varying from 0.358 for the lower-bound solution, to 0.379 for the upper-bound one. The corresponding distributions of the contact stresses are shown in Figure 3.a with a continuous line: over a significant length of the wall they are nearly coincident with the numerical solution. As a consequence, the distribution of the bending moments (Figure 3.b) is very close to the one computed with the finite-difference pseudo-static approach. It is also evident that the lower- and upper-bound solution are very close to each other for all practical purposes.

Figure 3(c,d) shows a further comparison in which the numerical results derive from the dynamic analysis, and are relative to the time instants that correspond to the attainment of the maximum bending moment in the wall. When these results are compared with those of the calculations based on limit equilibrium, only some minor discrepancies emerge, in the form of small differences in the contact stresses acting on the embedded length of the wall (Figure 5.c); these differences are probably due to the instantaneous acceleration field being non-uniform in the dynamic analysis, and result in a maximum bending moment which is only 15% larger than the one evaluated with the pseudo-static approach. The same figure shows also the results of a dynamic analysis in which the acceleration values of the Tolmezzo record were doubled ($a_{max} = 0.7$ g): it is remarkable that such an increase in the input acceleration produces only a very small increase in the bending moments. This shows unequivocally that, if the seismic input is severe enough to activate the above plastic mechanism, then the maximum internal forces do not depend from the intensity of the seismic input, but are related to the strength of the system only: the larger the strength (that is, the critical seismic coefficient, the larger the internal forces. As shown in Figure 3, a simple pseudo-static analysis of the plastic mechanism, based on limit equilibrium, is quite sufficient to evaluate the distribution of the internal forces under critical conditions.

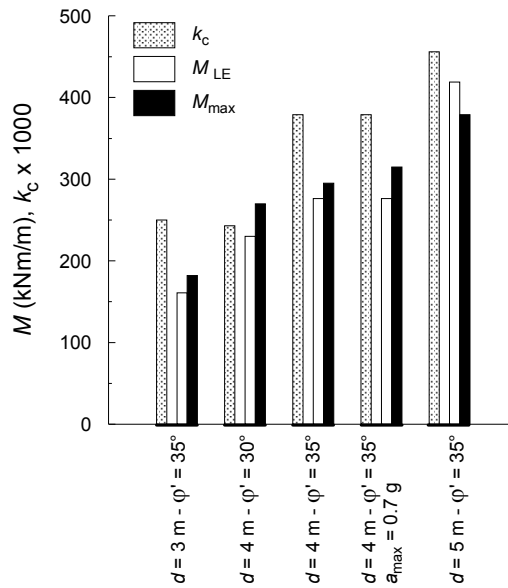


Figure 4. Summary of the maximum bending moments in the cantilevered wall and of the associated critical acceleration (from Callisto, 2014).

A parametric study carried out by Callisto (2014) indicated that this result is quite general, being replicable for different cantilevered walls schemes and not particularly dependent on the stiffness properties of the wall and the soil. As an example, the bar chart of Figure 4 shows the critical seismic coefficients computed with the pseudo-static iterative procedure and compares the corresponding maximum bending moments with those resulting from the numerical analyses. As a general result, it is evident that the internal forces increase with the critical seismic coefficient k_c . However, the cases with $d = 3\text{ m}$, $\varphi' = 35^\circ$ and with $d = 4\text{ m}$, $\varphi' = 30^\circ$ have a similar k_c but different internal forces, and the iterative limit equilibrium analysis is able to reproduce correctly this trend. These results are consistent with the basic assumption that, for an earthquake that is sufficiently intense to activate the plastic mechanism, the maximum internal forces depend on the strength of the system only, and that this strength can be expressed by the critical seismic coefficient.

Anchored walls

A further investigation employed the same tools discussed above to explore the behaviour of walls with a single level on anchors. The specific wall layout of Figure 2 was studied, with an excavation height of 5.5 m supported by a wall having an embedded length of 2 m and the anchor level located at a depth of 1.0 m. Three different anchor properties were devised, as reported in Table 1, where L_a is the active length of the anchor, T_{lim} is the equivalent strength of the anchor in plane strain conditions, and k_c is the critical seismic coefficient evaluated either from the FLAC pseudo-static analysis, or through an iterative pseudo-static (P.S.) limit equilibrium calculation, as discussed in the following.

Table 1. summary of the different anchor properties

Case	L_a (m)	T_{lim} (kN/m)	$k_c - \text{FLAC}$	$k_c - \text{P.S.}$
A	3.0	70	0.25	0.27
B	3.0	500	0.28	0.29
C	10.0	500	0.41	0.42

In case A, the anchor is relatively weak: the critical conditions evidenced by the a pseudo-static finite difference calculation is characterised by $k_c = 0.25$ and by the plastic mechanism shown in Figure 5: the anchor strength is fully mobilised and the wall rotates rigidly about a

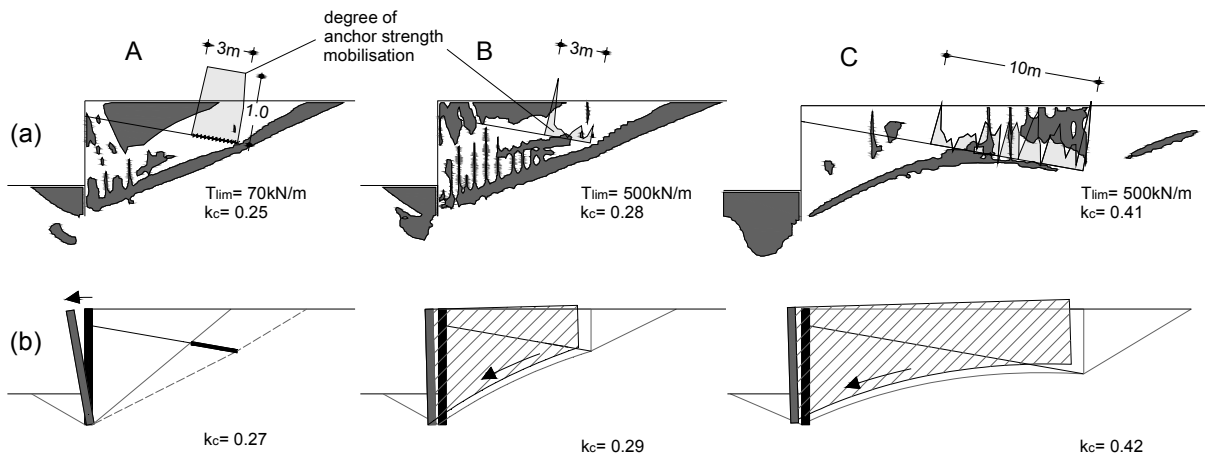


Figure 5. Anchored walls listed in Table 1: (a) contours of mobilised strength and (b) limit-equilibrium interpretation of the plastic mechanisms obtained with the numerical pseudo-static analyses.

point close to its toe. This case can be studied with a limit equilibrium calculation similar to that presented for the cantilevered scheme, in which however the wall is subjected to the known constant force T_{lim} . The critical seismic coefficient of 0.25 and the maximum bending moment of 118 kNm/m provided by the numerical pseudo-static calculation are well reproduced by this limit equilibrium approach.

However, for the schemes with stronger anchors the plastic mechanisms evidenced by the finite-difference calculations are quite different, entailing the mobilisation of the strength in a soil volume that includes the active part of the anchor. In other words, as the anchor becomes stronger, the critical seismic coefficient tends to increase, but this has the consequence of enlarging the size of the active soil wedge: when the active wedge extends to the location of the active anchor zone, the plastic mechanism assumes a global character.

For instance, progressing from case A to case B the geometry of the anchor does not change, but its strength increases by a factor of 7. However, the corresponding critical coefficient increases only from 0.25 to 0.28, because the anchor is short and a global mechanism is activated by seismic forces that are only slightly larger than in case A. On the contrary, in case C the anchor is stronger but also much longer than that of case A; therefore the global mechanism that develops because of the large resistance of the anchor is associated to a large critical seismic coefficient ($k_c = 0.42$).

The above global mechanisms were interpreted with a limit equilibrium approach that studies a rotational sliding along a log-spiral surface, as shown in Figure 5.b, assuming full mobilisation of the passive limit condition in front of the wall and of an active limit condition along a vertical surface passing through the terminal part of the anchor. This approach provides a satisfactory prediction of the critical seismic coefficient, as reported in Table 1 and in Figure 5, but is unable to provide the internal forces in the wall, since it analyses only the global equilibrium of the system.

Figure 6 provides an appreciation of the role of the local and global plastic mechanisms in determining the maximum internal forces in the wall. The figure shows the maximum bending moment M_{max} evaluated with the pseudo-static approach as a function of the critical seismic coefficient k_c . Points relative to cases A, B and C are marked in the figure, that however includes a larger number of results deriving from a parametric study. For local mechanisms, the maximum bending moment appears to increase linearly with k_c , and this trend can be obtained correctly also with a simple limit equilibrium calculation. These limit equilibrium

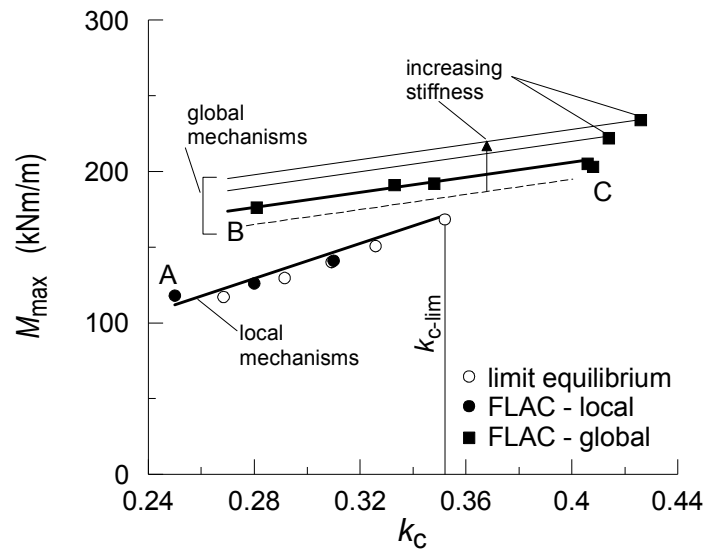


Figure 6. Summary of the maximum bending moments in anchored walls evaluated with the numerical pseudo-static analyses, plotted as a function of the critical seismic coefficient.

analyses show that for $k_c > k_{c-lim} \approx 0.35$ the critical seismic coefficient becomes independent of T_{lim} : for the present wall layout and soil strength, local mechanisms corresponding to critical seismic coefficients larger than this value are not possible, and any further increase in T_{lim} results in the activation of a global mechanism. However, a global mechanism can also be obtained for values of k_c smaller than k_{c-lim} when the anchor has a large resistance but a relatively short active length, as in case B.

For a given wall layout, Figure 6 shows that the maximum bending moments associated to the activation of global mechanisms are larger than those deriving from local mechanisms, and less variable with k_c . On the other hand, in a global mechanism the soil-wall contact surfaces are all internal to the soil volume delimited by the sliding surfaces, and therefore the soil-wall contact forces may depend on the stiffness properties of the wall, the soil and the anchor elements. This is shown in Figure 6 where, on the basis of a limited number of additional analysis, it is shown that the maximum bending moments in the wall increase with an increasing stiffness of the anchors. Full dynamic analyses were carried out also on anchored walls; for walls that under pseudo-static conditions activate a local plastic mechanism, the maximum internal forces show a trend similar to that of Figure 6, with values about 20 % larger. For wall layouts that activate global mechanisms, the significant effect of the stiffness of the system appears to be emphasized by the dynamic nature of the loads, but no clear trend has emerged yet.

Conclusions

This work gave attention to the maximum internal forces that may develop in an embedded retaining structure during an intense seismic motion. Through a combination of numerical analyses, carried out in pseudo-static and dynamic conditions, and simpler calculations based on limit equilibrium, it was shown that the principles of capacity design, that are aimed to provide the structural members with an intrinsic degree of safety, can be applied also to the earth retaining structures considered in this study, by interpreting their seismic behaviour as a sequence of successive activations of a relevant plastic mechanism. Hence, the maximum internal forces in the structural member can be derived from the analysis of the plastic mechanism and are related to the strength properties of the system rather than to the amplitude of the seismic actions.

The actual implementation of this design approach is limited to schemes in which the mobilisation of the strength of the soil is sufficient to activate a plastic mechanism. Retaining structures with multiple structural constraints would require the simultaneous mobilisation of the strength of the soil and of some structural component, following an adequate hierarchy; this appears feasible but is beyond the scope of the present work.

Cantilever retaining walls certainly fall in the category of structures for which the present approach is viable. In this case the plastic mechanism is well defined and easy to analyse, even with a simple spreadsheet calculation. The results of a large number of dynamic numerical analyses showed that the proposed method is consistent and reasonably accurate.

For anchored retaining walls the picture is made more complicated by the possibility that, for a given wall layout, different plastic mechanisms can be activated as an effect of a different geometry and resistance of the anchor level: for some values of the anchor resistance, the plastic mechanism can be either local or global; for larger resistances only global mechanisms can occur.

As a general result, for a given critical seismic coefficient the activation of a local mechanism corresponds to the lowest internal forces in the structure. Therefore, an advantageous design should prefer weak anchors (that is, with $k_c < k_{c-lim}$), located at a sufficient distance away from the wall, that should be able to mobilise their strength at the soil-bulb contact during a severe seismic event.

However, the actual strength of a grouted anchor is often quite difficult to estimate. Current design procedures tend to rely on empirical procedures and the actual anchor resistance is controlled only through pull-out tests carried out at a verification stage during the construction works. Therefore, it is very common that the actual anchor strength be underestimated at the design stage. This has the consequence that the actual internal forces in the wall during an earthquake can be significantly larger than those associated to a local mechanism. For instance, Figure 6 shows that for $k_c = 0.28$ a wall with a strong anchor undergoes a maximum bending moment which is about 40 % larger than that associated to a weak anchor. In this case, the possibility of carrying out pull-out test on full prototypes at the design stage would be highly beneficial, allowing a careful calibration of the most suitable anchor strength for the specific project.

REFERENCES

- Callisto (2014). Capacity design of embedded retaining structures, *Geotechnique*, 64, 204–2014. doi: <http://dx.doi.org/10.1680/geot.13.P.091>
- Callisto L and Soccodato FM (2010). Seismic design of flexible cantilevered retaining walls. *Journal of Geotechnical and Geoenvironmental Engineering*. 136(2):344-354, [http://dx.doi.org/10.1061/\(ASCE\)GT.1943-5606.0000216](http://dx.doi.org/10.1061/(ASCE)GT.1943-5606.0000216).
- Chang, M. F. (1981). Static and seismic lateral earth pressures on rigid retaining structures. PhD thesis, School of Civil Engineering, Purdue University, West Lafayette, IN, USA.
- Itasca (2005). *FLAC Fast Lagrangian Analysis of Continua v. 5.0. User's Manual*.
- Lancellotta R (2007). Lower-bound approach for seismic passive earth resistance. *Géotechnique* 57(3): 319-321.
- Masing, G. (1926). Eigenspannungen und Verfertigungsbim Messing. Proceedings of the 2nd international congress on applied mechanics, pp.322–355. Zurich-Leipzig: Füssli (in German).
- Seed, H. B. & Idriss, I. M. (1979). Soil moduli and damping factors for dynamic analysis, Report No. EERC70-10. Berkeley, CA, USA: University of California.